



Proceedings Article

A High Resolution Permanent Magnet Magnetic Particle Imaging Device

Ning He ^{a,b,c} · Chenxiao Xu^{a,b,c} · Zhonghao Zhang^{a,b,c} · Jiawei Hu^{a,b,c} · Lei Li ^{a,b,c} ·
Qibin Wang^{a,b,c} · Pengyue Guo^{a,b,c} · Yunpeng Gao^{a,b,c} · Yidong Liao^{a,b,c} · Dawei Ge^{a,b,c} ·
Chenglong Shi^{a,b,c} · Man Luo^{a,b,c} · Shouping Zhu ^{a,b,c,*}

^aSchool of Life Science and Technology, Xidian University & Engineering Research Center of Molecular and Neuro Imaging, Ministry of Education, Xi'an, Shaanxi 710126, China

^bXi'an Key Laboratory of Intelligent Sensing and Regulation of trans-Scale Life Information & International Joint Research Center for Advanced Medical Imaging and Intelligent Diagnosis and Treatment, School of Life Science and Technology, Xidian University, Xi'an, Shaanxi 710126, China

^cInnovation Center for Advanced Medical Imaging and Intelligent Medicine, Guangzhou Institute of Technology, Xidian University, Guangzhou, Guangdong 51055, China

*Corresponding author, email: spzhu@xidian.edu.cn

© 2023 He *et al.*; licensee Infinite Science Publishing GmbH

This is an Open Access article distributed under the terms of the Creative Commons Attribution License (<http://creativecommons.org/licenses/by/4.0>), which permits unrestricted use, distribution, and reproduction in any medium, provided the original work is properly cited.

Abstract

Magnetic particle imaging (MPI) is a novel emerging tomographic technique with high resolution and high sensitivity. Typically, the magnetic fields of MPI scanners are generated by current-carrying coils, resulting in an immense power consumption and making it difficult to apply in clinical research. The MPI device based on a Halbach array provides a new solution. In this work, a mechanically driven scanning MPI device was designed using a Halbach permanent magnet array. The device consists of four layers of Halbach arrays, and is ultimately capable of achieving a FOV of 70 mm diameter, and a resolution better than 0.5 mm. Compared with the previous Halbach permanent magnet MPI device, this device generates field-free point (FFP) at which the field strength increases in all spatial directions. Moreover, the stability of the structure was analyzed by structural mechanics calculations and magnetic field error simulations, and the feasibility of the device was analyzed by simulations of the system scan trajectory and image reconstruction.

1. Introduction

Magnetic particle imaging (MPI), is a new emerging medical imaging technology, which can image the distribution of superparamagnetic iron-oxide nanoparticles (SPIOs) [1]. Since the introduction of MPI in 2005, MPI has been widely used in bioimaging. However, the immense power consumption has limited its upgrade to clinical. The first mechanically driven MPI device was proposed by Harbi et al, which drives the FFP movement by rotating the drive field, and the device can drastically

reduce the power consumption [2]. A novel structure of MPI was presented by Bakenecker et al, which structure consists of two layers of $k=2$ Halbach arrays forming the selection field and two layers of $k=1$ Halbach arrays generating the drive field, and this device can achieve 2D imaging [3].

Based on the previous study, we propose a permanent magnet device for 3D imaging, which consists of four Halbach arrays. The device generates a high gradient selection field and a high field strength drive field, providing high-resolution imaging and large field scan-

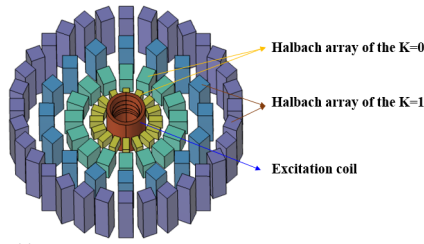


Figure 1: The Halbach-MPI setup. Halbach array of the $k=1$ generates the drive field. Halbach array of the $k=0$ generates the selection field offering a high gradient.

ning. The device's power consumption is much lower than the current-carrying coils device of the same FOV.

II. Methods and materials

We used two layers of nested $k=0$ Halbach arrays for generating selection fields and two layers of $k=1$ Halbach arrays for generating drive fields, as shown in Figure 1. Halbach arrays have different morphologies defined by block magnetization direction and block distribution angle [4, 5]. This structure produces a high gradient field and a homogeneous drive field. The high gradient field will allow for high resolution of the device, and the drive field moves the FFP on a 2D trajectory. This device allows 3D imaging by continuously shifting the phantom position along the y-axis. This device uses the excitation coil induced magnetic particle response signal. The device's diameter is 512 mm, the length is 260 mm and the bore-size is 100 mm.

II.I. Selection field

Figure 1 shows the selection field. We used two layers of nested $k=0$ Halbach arrays for generating a high gradient field. The selection field generates an FFP at which the field strength increases in all spatial directions. The gradient strength of the selection field is 4 T m^{-1} , which will allow for high resolution imaging.

II.II. Drive field

Figure 1 shows the drive field. We used two layers of nested $k=1$ Halbach arrays for generating a homogeneous magnetic field, which can ideally drive the FFP for scanning. The magnetic flux density of the drive field varies with the rotation angle, ranging from 0~170 mT. The magnetic flux density of the drive field can be adjusted by the rotation angle between the two Halbach arrays. The driving field drives the FFP to achieve two scanning trajectories [3, 6, 7], radial trajectory, and flower trajectory.

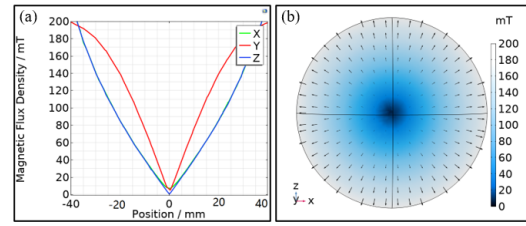


Figure 2: Simulation of the Selection field. (a) Selection field flux density distribution, linear range -40 mm to 40 mm , the gradient of the selection field is 4 T m^{-1} ; (b) Selection field flux density distribution, distribution radius $r=35 \text{ mm}$.

II.III. Magnet force analysis

The Halbach MPI setup is composed entirely of permanent magnets, so the whole structure will be subjected to very large magnetic forces. The forces are calculated according to the Maxwell surface stress tensor [8].

$$\partial \cdot F / \partial \cdot V = \nabla \cdot T. \quad (1)$$

$$T_{ij} = B_i \cdot B_j / \mu_0 - \delta_{ij} B^2 / 2 \cdot \mu_0. \quad (2)$$

With F the magnetic force magnitude, V the volume size of the object under stress, T_{ij} the Maxwell stress tensor, $B_i B_j$ the magnetic flux density in different dimensions, δ_{ij} the Kronecker symbol, B the matrix of magnetic flux density.

II.IV. Error analysis methods

The Halbach MPI setup is a fully mechanically driven device, so the impact of various errors needs to be considered. In this device, we analyzed the error simulation of the overall structure. The Halbach MPI structural design was standardized by analyzing the error induced by magnetic field variation.

III. Results

In this device, the simulation of the magnetic field, force calculation, and error simulation were based on COMSOL Multiphysics (Version 5.6, COMSOL AB, Stockholm, Sweden), and image reconstruction was performed using Python 3.7.

III.I. Simulation of magnetic field

Figure 2 shows the simulation result of the selection field. Figure 3 shows the simulation result of the drive field. Simulations have shown that the device can achieve a FOV of 70 mm in diameter.

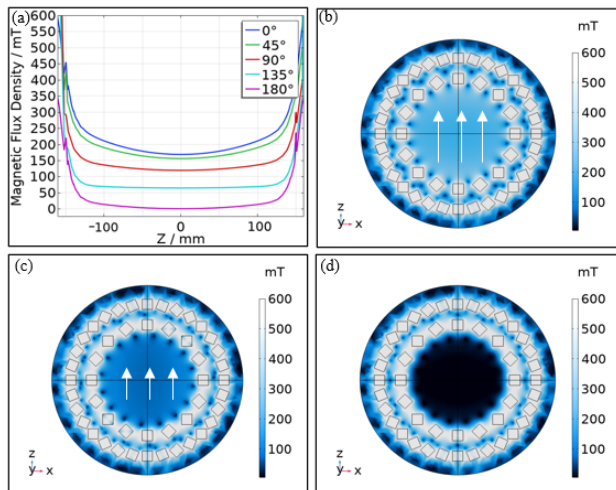


Figure 3: Simulation of the drive field. (a) Variation of magnetic flux density of the driving field with the rotation angle, with the range from 0–170 mT. (b) Flux density distribution when the rotation angle is 0°. (c) Flux density distribution when the rotation angle is 90°. (d) Flux density distribution when the rotation angle is 180°.

III.II. Analysis of magnetic force and error

In this device, we have made a force analysis of the structure in Figure 1. The resultant surface has different force magnitudes for each angle during the rotation of the drive field, where the maximum magnetic field force is about 1500 N and the maximum torque to be provided during the rotation is 400 Nm.

It was found that when the dimensional error was greater than 1 mm, the magnetic field uniformity decreases by 3.86%, thus reducing the performance of the device. When the axial movement of the block was greater than 2 mm, the selection field error exceeds 3.00%. When the radial movement of the block was greater than 1 mm, the gradient field error exceeds 2.85%.

III.III. Image reconstruction

In this experiment, We used the X-space method for image reconstruction. We analyzed the imaging effect of different scanning trajectories and the resolution of the system by the different spacing of phantoms. The experiments were performed with magnetic particles of 40 nm diameter, excitation field frequency of 25 kHz and amplitude of 5 mT. The results as shown in Figure 4 and Figure 5.

IV. Conclusion

In this device, we proposed a nested structural Halbach MPI setup with a large imaging field of view, high mag-

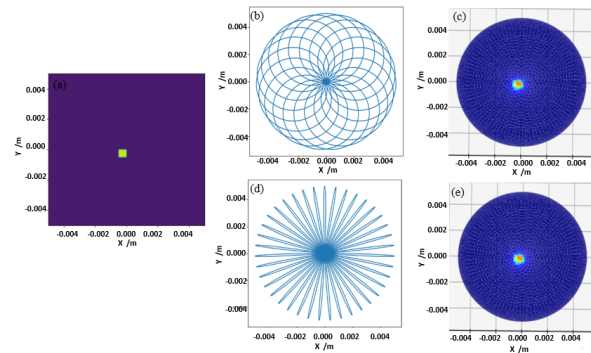


Figure 4: Imaging analysis of different scanning trajectories. (a) square phantom, the size of 0.5 mm×0.5 mm; (b) radial-shaped trajectory; (c) Image reconstruction based on X-space method; (d) flower trajectory; (e) Image reconstruction based on X-space method.

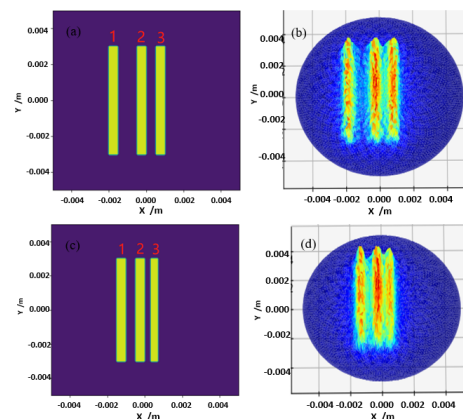


Figure 5: Image reconstruction using line phantoms with different distance. (a) 1 and 2 spacing of 1 mm, 2 and 3 spacing of 0.5 mm; (b) Image reconstruction based on X-space method; (c) 1 and 2 spacing of 0.5 mm, 2 and 3 spacing of 0.3 mm; (d) Image reconstruction based on X-space method.

netic gradient fields and low energy consumption. Based on this device, high-resolution imaging in 3D can be achieved. In future work, we will use the device for vascular imaging.

Acknowledgments

This work was supported by the National Natural Science Foundation of China under Grant Nos. 62027901, 62071362, 82272050, 61901342, the Natural Science Basic Research Program of Shaanxi Province under Grant Nos. 2021JZ-29, 2021SF-131, 2021SF-169, and the Fundamental Research Funds for the Central Universities under Grant No. JB211205.

Author's statement

Conflict of interest: Authors state no conflict of interest.

References

- [1] B. Gleich and J. Weizenecker. Tomographic imaging using the non-linear response of magnetic particles. *Nature*, 435(7046):1214–1217, 2005, doi:[10.1038/nature03808](https://doi.org/10.1038/nature03808).
- [2] C. Kierans, H. Bagheri, K. J. Nelson, B. A. Andrade, C. L. Wong, A. Frederick, and M. E. Hayden. A mechanically driven magnetic particle imaging scanner. *Applied Physics Letters*, 2018.
- [3] A. Bakenecker, J. Schumacher, P. Blümmler, K. Gräfe, M. Ahlborg, and T. Buzug. A concept for a magnetic particle imaging scanner with halbach arrays. *Physics in Medicine & Biology*, 65(19):195014, 2020.
- [4] P. Blümmler. Magnetic guiding with permanent magnets: Concept, realization and applications to nanoparticles and cells. *Cells*, 10(10):2708, 2021.
- [5] L. Mirzozan, M. A. Rückert, C. Greiner, A. von Boehn, T. Kampf, V. C. Behr, and P. Vogel. Fully mechanically driven traveling wave mpi. *International Journal on Magnetic Particle Imaging*, 8(1 Suppl 1), 2022.
- [6] H. Bagheri, C. Kierans, K. Nelson, B. Andrade, C. Wong, A. Frederick, and M. Hayden. A mechanically driven magnetic particle imaging scanner. *Applied Physics Letters*, 113(18):183703, 2018.
- [7] C. B. Top, A. Güngör, S. Ilbey, and H. E. Güven. Trajectory analysis for field free line magnetic particle imaging. *Medical Physics*, 46(4):1592–1607, 2019.
- [8] M. Javid and P. M. Brown, *Field Analysis and Electromagnetics*. Courier Dover Publications, 2019,